Article

Not peer-reviewed version

Study on a Thermally Crosslinking Clay-Free Weak Gel Water-Based Drilling Fluids

Taifeng Zhang , Jinsheng Sun , Kaihe Lv , Jingping Liu * , Lei Nie , Yufan Zheng , Yuanwei Sun , Ning Huang , Delin Hou , Han Yan , Yecheng Li

Posted Date: 26 February 2026

doi: 10.20944/preprints202602.1654.v1

Keywords: clay-free water-based drilling fluids; three-dimensional network; weak gel; hightemperature; high-salinity; thermal crosslinking

 doi:10.20944/preprints202602.1654.v1

Article

Study on a Thermally Crosslinking Clay-Free Weak Gel Water-Based Drilling Fluids

Taifeng Zhang [1,2], Jinsheng Sun [1,2], Kaihe Lv [1,2], Jingping Liu [1,2,*], Lei Nie [1,2], Yufan Zheng [1,2], Yuanwei Sun [1,2], Ning Huang [1,2], Delin Hou [1,2], Han Yan [1,2] and Yecheng Li [1,2]

[1] State Key Laboratory of Deep Oil and Gas, China University of Petroleum (East China), Qingdao, 266580, Shandong, China

[2] School of Petroleum Engineering, China University of Petroleum (East China), Qingdao, 266580, Shandong, China

* Correspondence: liujingping20@126.com

Abstract

In this study, a thermally crosslinking clay-free weak gel water-based drilling fluid based on salt-responsive polymers and crosslinking agents was investigated, a promising and feasible strategy. Firstly, a salt-tolerant polymer was synthesized using N, N-dimethylacrylamide (DMAA), [2-(methacryloyloxy)ethyl]dimethyl-(3-sulfonopropyl) ammonium hydroxide (DMAPS), and acrylamide (AM). $BPEI_{10000}$ was selected as the thermal crosslinking agent. The optimal crosslinking could be achieved at 180 °C and 36% NaCl when the RMFL concentration was 2.0%, and the $BPEI_{10000}$ concentration was 0.1%. Performance evaluation demonstrated that the crosslinking between RMFL and $BPEI_{10000}$ could enhance the AV, PV, and YP of the RMFL($BPEI_{10000}$)/CF-WBDFs after aging at 180 °C for 16 h, and reduce FL_{API}. The RMFL($BPEI_{10000}$)/CF-WBDFs exhibited appropriate shear-thinning behavior, viscoelasticity, thixotropy, and recoverable viscosity under high-temperature, high-salinity, and high-pressure conditions. Mechanism analysis revealed that RMFL and $BPEI_{10000}$ could form a predominantly negatively charged, three-dimensional crosslinking weak gel at high temperatures. The crosslinking weak gel could form dense filter cakes, improving rheological properties and reducing filtration loss of CFWBDFs in high-temperature, high-salinity environments. This paper proposed a novel method to address the technical challenge of rheological performance failure of CFWBDFs, offering valuable insights for subsequent investigations.

Keywords: clay-free water-based drilling fluids; three-dimensional network; weak gel; high-temperature; high-salinity; thermal crosslinking

1. Introduction

Oil and natural gas are essential energy sources on which human societies depend. They will continue to play a key role in the energy landscape for the foreseeable future. As the pace of oil and gas exploration and development speeds up, shallow and medium-depth reservoirs are becoming increasingly depleted. Deep and ultra-deep oil and gas account for about 34% of total geological resources worldwide, representing abundant, high-potential resources. The deep and ultra-deep resources are a viable alternative energy source in the future, making exploration and development of deeper layers an inevitable trend in the oil and gas industry [1]. Drilling is the first process in deep oil and gas development and remains the central engineering in exploration and production.

However, the harsh geological conditions at greater depths posed significant obstacles to drilling engineering. Drilling fluids are the circulating working fluids used in drilling operations, such as balancing formation pressure, maintaining wellbore stability, suspending cuttings, and lubricating drill bits. Safe and efficient deep drilling requires high-performance drilling fluids [2]. Drilling fluids are generally classified into water-based and oil-based systems. Oil-based drilling fluids provide better resistance to high temperatures and high salinity. They are the preferred choice for drilling

 doi:10.20944/preprints202602.1654.v1

through harsh formations. However, oil-based drilling fluids have several shortcomings, including cost, environmental pollution, and difficulty in recycling. Drilling engineers are increasingly concerned about water-based drilling fluids due to their lower cost and environmental advantages. Clay-free water-based drilling fluids (CFWBDFs) do not contain clay-based materials. They offer better reservoir protection and faster drilling speeds. CFWBDFs can avoid the negative effects of clay aggregation or dispersion on their performance, particularly under high-temperature and high-salinity conditions. Therefore, CFWBDFs present promising opportunities for research and applications [3]. However, rheological modifiers are prone to failure under high-temperature and high-salinity conditions. The rheological properties of CFWBDFs will deteriorate, leading to serious downhole problems, such as stuck pipe and wellbore collapse. Severe accidents will prevent the safe and efficient production of deep oil and gas.

Rheology modifiers for CFWBDFs are mainly classified into modified natural materials and synthetic polymers. Ali [4] developed a lignin-based biopolymer (BioDrill FM400) that served as a rheology modifier and fluid-loss reducer. The temperature resistance of BioDrill FM400 was 150 °C. When BioDrill FM400 was blended with xanthan gum (XC), it could effectively improve PV, YP, and gel strength of CFWBDFs. Li et al.[5] used tara gum as a rheology modifier in solid-free water-based drilling fluids (SFWBDFs), and the SFWBDFs achieved a temperature resistance of 140 °C. Liu [6] prepared a hydrophobic-modified hydroxyethyl cellulose (HMHEC) as a rheology modifier. HMHEC also exhibited superior high-temperature resistance and high-salinity tolerance, with improved rheological control properties compared to PAM and XC, which made HMHEC a green, sustainable alternative to traditional rheology modifiers in CFWBDFs. Ali et al. [7] used carboxymethyl cassava starch (CMTS) as a rheology modifier and filtration loss in CFWBDFs. The high-temperature, high-pressure filtration loss ($FL_{HTHP(126\ °C,\ 500\ psi)}$) was reduced to 11.0 mL at a CMTS concentration of 2.29 wt%. Although modified natural materials are widely available and environmentally friendly, they contain plenty of ether, glycosidic, and ester bonds that easily degrade at higher temperatures (150 °C). Even when sulfonation, grafting, crosslinking, and other chemical modification strategies are employed to enhance the thermal resistance of the materials up to 180 °C, such improvements are often achieved at the expense of complex processing procedures and high costs. Due to insufficient thermal stability, existing naturally modified materials cannot be applied in deep formations.

Synthetic polymers offer high design flexibility, with adjustable numbers and types of functional groups and molecular weights [8]. Rheology modifiers with high-temperature and high-salinity resistance could be developed by copolymerizing vinyl monomers using hydrophobic, crosslinking, and zwitterionic modifications [9]. Davoodi [10]synthesized a hydrophobic copolymer (SBASC). Under 25.0% NaCl and 5.7% KCl composite salt conditions, CFWBDFs containing 1% SBASC showed higher PV and YP after aging at 121 °C, with FL_{API} and FL_{HTHP} decreasing by 38.8% and 47.5%. Zhang [11] developed a hydrophobic associative polymer (SSZN). SSZN displayed excellent compatibility with xanthan gum, white bitumen, and modified starch. The CFWBDFs exhibited the PV of 87.0 mPa·s, YP of 11.5 Pa, and $FL_{HTHP(150\ °C,\ 3.5MPa)}$ was 9.7 mL after aging at 150 ° C. Wang [12] synthesized a zwitterionic thickener (FPOD), which showed good compatibility in saturated calcium bromide($CaBr_2$) completion fluids. When the concentration of FPOD was 1% in saturated $CaBr_2$ completion fluids, the AV was 37.0 mPa·s after aging at 150 °C. Xie et al. [13] synthesized a viscosifier (SDKP) for CFWBDFs. SDKP exhibited temperature resistance up to 160 °C and salt resistance up to 15% NaCl. After aging at 160 °C, the CFWBDFs containing 1% SDKP exhibited an AV of 56.0 mPa·s, PV of 37.0 mPa·s, YP of 19.0 Pa, and $FL_{HTHP\ (120\ °C,\ 3.5\ MPa)}$ of 12.8 mL. Although existing polymers exhibit good thermal resistance (up to 160 °C) and salt tolerance (up to 15% NaCl), they do not perform effectively at 180 °C and saturated NaCl conditions.

Most polymers are prone to degradation at high temperatures, including scission of main and side chains, leading to failure of their thickening properties. Especially in high-salinity environments, a large amount of electrolytes compresses the diffuse double layer of polymers, causing the polymer chains to curl and further weakening their rheology-modifying ability. Although slightly crosslinked,

 doi:10.20944/preprints202602.1654.v1

hydrophobic and zwitterionic modifications can enhance the thermal and salt resistance of polymers. However, these measures still cannot prevent thermal degradation of polymers at high temperatures. Ultimately, the rheological performance of clay-free water-based drilling fluids deteriorates. Therefore, it is urgent to seek a novel approach to enhance the salt tolerance and high-temperature stability of polymers. Cui improved the temperature resistance of polyacrylamide from 140 °C to 200 °C using the "Crosslinking compensation" method [14]. "Crosslinking compensation" involves crosslinking polymers with crosslinkers at high temperatures to combat polymer hydrolysis and degradation, thereby maintaining the rheological properties of drilling fluids. Therefore, under the guidance of the "crosslinking compensation" method, we can design a salt-tolerant polymer and crosslink it with a crosslinking agent at high temperature to mitigate polymer degradation, thereby enabling rheological control of clay-free water-based drilling fluids under high-temperature and high-salinity conditions[15].

In this study, a thermally crosslinking clay-free weak gel water-based drilling fluid was formulated with a salt-resistant rheology modifier RMFL and a crosslinking agent polyethyleneimine (PEI). We preliminarily investigated the effect of thermal crosslinking between RMFL and PEI on the properties of clay-free water-based drilling fluids, providing a new perspective for the design of rheology modifiers, drilling fluid formulation, and performance regulation.

2. Results and Discussion

2.1. Effect of DMAM and DMAPS on the Salt Resistance of Polymers

Polyacrylamide (PAM) is a thickening agent widely used in oilfield operations, including drilling, profile control, water blocking, oil displacement, and fracturing [16]. However, PAM's resistance to high temperature and salinity was insufficient. N, N-Dimethylacrylamide contains rigid dimethyl groups, providing better temperature resistance than AM. The steric hindrance from these dimethyl groups increases intermolecular repulsion, preventing polymer chains from curling and from hydrolysis in high-temperature, high-salinity environments. DMAA is more suitable than AM as a backbone for high-temperature and high-salinity-resistant polymers [17–19]. Zwitterionic polymers are polyelectrolytes that contain both cationic and anionic groups. In electrolyte solutions, electrostatic repulsion between these groups is shielded, allowing polymer chains to fully extend. This results in increased drilling fluid viscosity and shear strength, thereby enhancing rheological properties [20]. The effects of PAM, PDMAA, and PDMASs on solution properties were evaluated at different NaCl concentrations, with a polymer concentration of 3.0 wt%.

As shown in Figure 1(a)-(d), the AV, PV, and YP of the PAM/CFWBDFs reduced significantly with increasing NaCl concentration from 0% to 36%. As shown in Figure 2(d), the FL_{API} of the PAM solution increased with increasing NaCl concentration, with all filtration losses observed at 25% NaCl. Under positive pressure, the polymers could form filter cakes that seal micropores and microcracks. A higher polymer molecular weight or larger hydrodynamic volume enhanced the sealing effect on micro/nanopores within the filter cake, resulting in a dense cake and less filtration loss [21]. Greater molecular weight also strengthened the binding effect of highly hydrating groups (such as amide and sulfonate groups) on free water, further reducing the filtration loss. PAM has good viscosity-increasing properties in freshwater. However, a higher concentration of Na^+ caused PAM chains to curl, weakening the viscosity enhancement and the filtration loss reduction properties. Surprisingly, there were no significant declines in AV, PV, or YP of PDMAA/CFWBDFs with increasing NaCl concentration, and higher NaCl concentrations did not increase FL_{API}. It was indicated that PDMAA exhibited better salt tolerance than PAM. From Figure 1(e)-(h), it was clear that the AV of PDMAS/CFWBDFs increased as the NaCl concentration rose after adding the DMAPS to the PDMAA molecular chains. The PV stayed within a narrow range of 40.0 to 48.0 mPa·s, and the YP ranged from 9.5 to 16.5 Pa. When the mass fraction of DMAPS was 1.0 wt%, there was the best performance of PDMAS compared to PDMAA.

 doi:10.20944/preprints202602.1654.v1

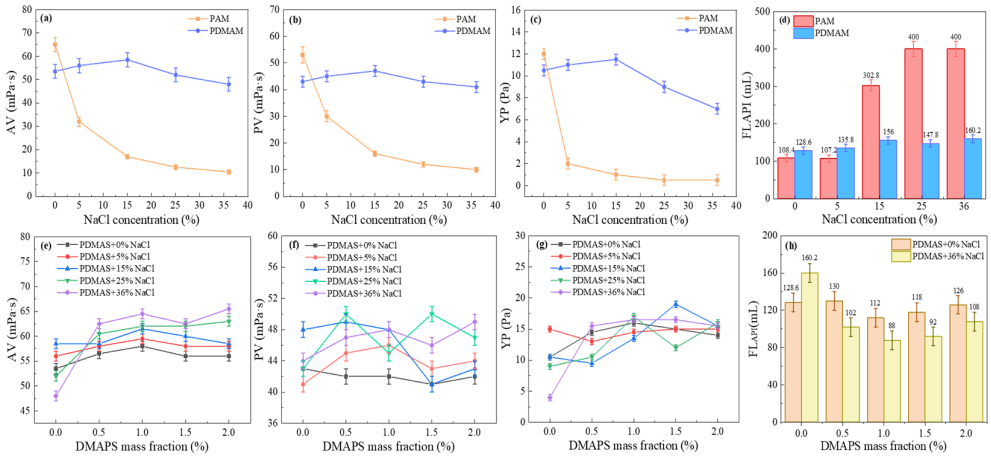

Figure 1. Influence of DMAA and zwitterionic side-chain DMAPS on the salt resistance of polymers. (a)-(d) Comparison of the viscosity-enhancing and filtration-loss reduction abilities of PDMAM and PAM at different NaCl concentrations; (e)-(h) Effect of DMAPS mass fraction on the viscosity enhancement and filtration-loss reduction of PDMAS at different NaCl concentrations.

As shown in Figure 2(a), the transmittance of the PDMAA/CFWBDFs decreased steadily with increasing NaCl concentration. The transmittance of PDMAS/CFWBDFs remained mainly stable at around 70%. The PDMAM/CFWBDFs became slightly turbid as NaCl concentration increased, while the PDMAS/CFWBDFs shifted from clear to slightly turbid. This phenomenon may be due to the formation of hydrophobic regions by PDMAM and PDMAS within the solutions, leading to decreased light transmittance [22].

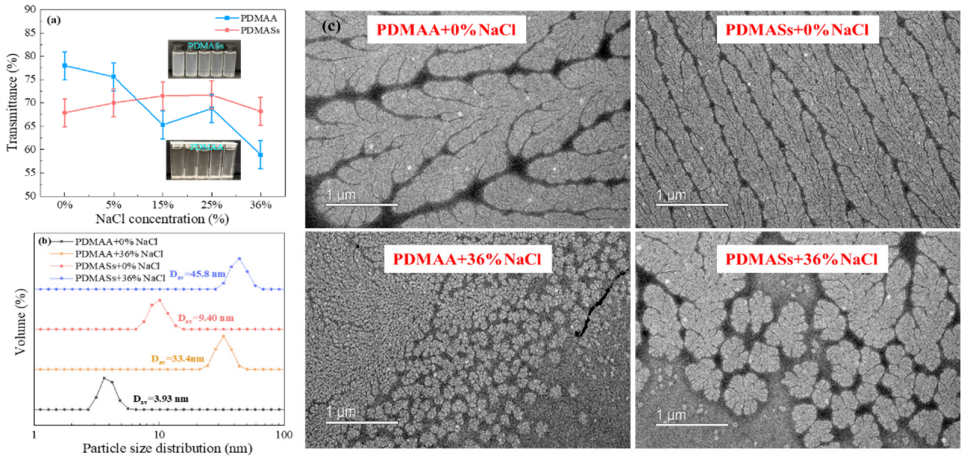

Figure 2. Microscopic mechanism analysis of the salt tolerance of PDMAA and PDMASs. (a) Solution transmittance analysis;(b) Polymer particle size analysis; (c) Polymer micromorphology analysis.

From Figure 2(b), it was shown that at 0% NaCl, the average particle sizes (D_{av}) of PDMAA and PDMAS were 3.93 nm and 9.40 nm, respectively. At 36% NaCl, D_{av} increased to 33.4 nm for PDMAA and 45.8 nm for PDMAS. It suggested that NaCl promoted polymer extension, allowing polymers to adsorb more water, and the D_{av} of polymers was enlarged.

As shown in Figure 2(c), both PDMAA and PDMAS had slender, willow-like shapes at 0% NaCl. More side chains were stretching out; the polymers were fully extended in a high-salinity environment. After the polymer chains extended, they enhanced the interpolymer interactions, thereby forming a three-dimensional associative network. The network likely resulted from weak

 doi:10.20944/preprints202602.1654.v1

hydrophobic interactions of dimethyl groups in DMAA. A higher concentration of Na+ increased the polarity of the solutions and promoted hydrophobic association among a small number of dimethyl groups, resulting in the formation of a three-dimensional associative network [23]. Undoubtedly, PDMAA/CFWBDFs exhibited higher AV, PV, and YP and lower FL_{API} than PAM/CFWBDFs under high-salinity conditions. In addition, PDMASs possessed betaine side chains, which extended and resulted in a larger hydrodynamic radius in a high-salinity environment [24], thereby enhancing AV, PV, and YP, and reducing filtration loss.

2.2. Effect of AM Mass fraction on the Properties of the Crosslinked System

Polyethyleneimine was introduced to crosslink polymers via transamidation reactions at high temperatures, preventing polymer degradation and performance failure due to high-temperature hydrolysis. Polyethyleneimine (PEI) is an aziridine polymer containing abundant imine groups. These imine groups are highly reactive and easily crosslink with functional groups in polymers, such as amide, carboxyl, or hydroxyl groups. PEI is often used as the crosslinker in oilfield operations, including profile adjustment, water blocking, and fracturing [25]. The number of amide groups, which serve as crosslinking sites, will influence the crosslinking efficiency between the polymer and PEI. Under conditions of 180 °C and 36% NaCl, the crosslinked product between synthesized polymers (PDMASA-0, PDMASA-1, PDMASA-2, PDMASA-3, and PDMASA-4) and 0.25wt%(w/v) $LPEI_{1800}$ after aging was observed. The rheological and filtrate loss properties of each sample were evaluated.

As shown in Figure 3. From Figure 3(a)-(e), under 36% NaCl conditions, PDMASA-0($LPEI_{1800}$)/CFWBDFs and PDMASA-1($LPEI_{1800}$)/CFWBDFs appeared milky white and highly diluted after aging at 180 °C. In contrast, many macroscopic gel particles existed in the PDMASA-2($LPEI_{1800}$)/CFWBDFs and PDMASA-3($LPEI_{1800}$)/CFWBDFs. Surprisingly, the PDMASA-4($LPEI_{1800}$)/CFWBDFs formed a gel that did not flow after aging [26]. As demonstrated in Figure 3(f)-(h), under 180 °C and 36% NaCl conditions, the combining systems of PDMASA-0, PDMASA-1, PDMASA-2, and PDMASA-3 with 0.25wt%$LPEI_{1800}$ exhibited the AV of 6.0 to 8.0 mPa·s, the PV of only 5.0 to 7.0 mPa·s, and the YP of only 1.0 Pa. The weakly gel formed by PDMASA-4 and $LPEI_{1800}$ became a flowable viscous solution after shearing, with the AV of 66.0 mPa·s, the PV of 52.0 mPa·s, and the YP of 14.0 Pa. The results suggested excessive crosslinking between PDMASA-4 and $LPEI_{1800}$.

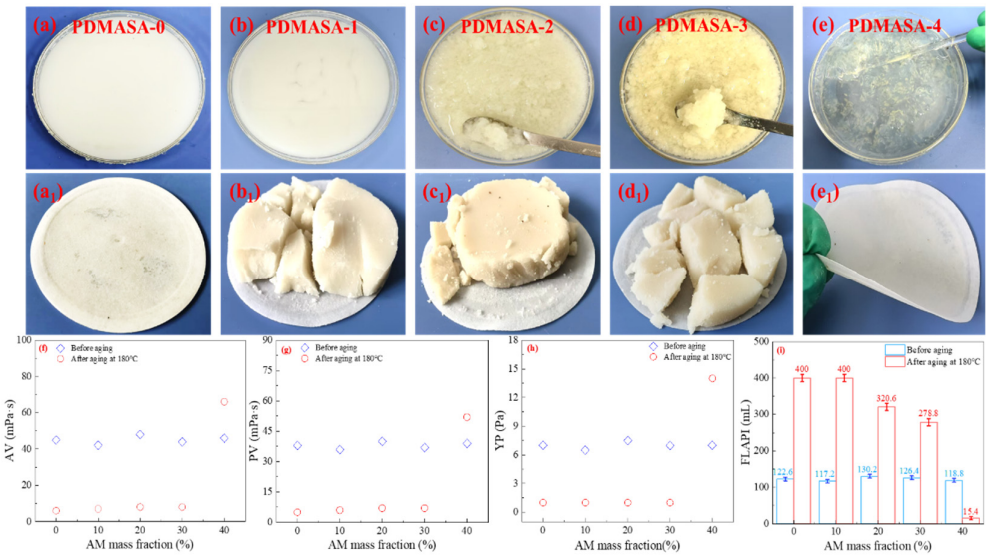

Figure 3. Effect of AM mass fractions on the properties of the crosslinked system under 36% NaCl and 180 °C conditions. (a)-(e) the appearance of the polymers and the $LPEI_{1800}$ crosslinked system after aging; (a_1)-(e_1) Appearance of the filter cakes of crosslinked systems; (f)-(i) AV, PV, YP of polymer($LPEI_{1800}$)/CFWBDFs.

 doi:10.20944/preprints202602.1654.v1

From Figure 3(i), it was clear that the FL_{API} of systems from Figure 3(a) to (d) are 350.0, 350.0, 320.6, and 278.8 mL, respectively. However, the FL_{API} of the system shown in Figure 2(e) was only 15.4 mL.

The filter cakes from each system are shown in Figure 3 (a_1). The PDMASA-0(LPEI$_{1800}$)/CFWBDFs had a thinner filter cake but experienced significant filtration loss. It was suggested that PDMASA-0, lacking amide groups, could not crosslink with LPEI$_{1800}$ at high temperatures. The filter cakes of the CFWBDFs shown in Figure 3(b_1)-(d_1) were thicker, with a large amount of filtration loss, indicating that the water-insoluble gel particles were formed by PDMASA-1, PDMASA-2, and PDMASA-3 crosslinking with LPEI$_{1800}$.It confirmed that PDMASA-1, PDMASA-2, and PDMASA-3 could crosslink with LPEI$_{1800}$. However, the gel particles could not effectively improve the rheological properties or reduce the filtration loss.

After PDMASA-4 crosslinking with LPEI$_{1800}$, the viscous solution could be obtained. It showed increased AV, PV, and YP and a decreased FL_{API}. As shown in Figure 3(e_1), the filter cake was thin, with no visible gel particles on its surface [27]. The results indicated that adding 0.25% LPEI$_{1800}$ (m/v) with an AM mass fraction of 40 wt% to PDMASA polymerization enabled PDMASA and LPEI$_{1800}$ to crosslink [28]. Even with excessive crosslinking, it still aligned with our predicted model. Therefore, the optimal mass fraction for AM polymerization was 40 wt%.

2.3. Preparation and Characterization of RMFL

The preparation method is shown in Figure 4. The synthesis route was illustrated in the above section. The characterization of RMFL is shown in Figure 5. The infrared spectrum is shown in Figure 5(a). The characteristic peak at 3388 cm^{-1} was from N-H stretching in the amide groups; the peaks at 2924 and 2870 cm^{-1} from C-H stretching in methyl and methylene groups [29]; the peaks at 1671 cm^{-1} were from the C=O stretching in the amide groups; the peak at 1615 cm^{-1} was from N-H bending vibration; the peak at 1450 cm^{-1} was from the N^+-C stretch in the quaternary ammonium cation; the peaks at 1180 cm^{-1} and 1037 cm^{-1} were from S=O and S-O stretching in the sulfonic acid group; the peak at 628 cm^{-1} was from C-S stretching [30]. Infrared spectroscopy analysis indicated that the product contained amide, methyl, carbonyl, quaternary ammonium, and sulfonic acid groups.

The ^1H NMR spectrum is shown in Figure 5(b), the peak at 1.11 ppm was attributed to the chemical shift of H on the methyl groups attached to the polymer main chains; the peak at 1.53 ppm was from the chemical shift of H in the methylene groups of the main chains; multiple peaks between 1.60 and 1.80 ppm originated from the chemical shift of H on the methylene groups within the main chain[31]; the peak at 2.27 ppm came from the chemical shift of H on the intermediate methylene group of N+-CH_2-CH_2-CH_2-SO_3[32]; The peaks from 2.80 to 3.20 ppm correspond to the chemical shift of H on -$CON(CH_3)_2$; the peak at 3.20 ppm was related with the chemical shift of H in N+$(CH_3)_2$; and the peak at 3.28 ppm corresponded to the chemical shift of H in N+-CH_2; the peak at 3.56 ppm resulted from the chemical shift of H in the methylene bridge connected to the sulfonate group within N+-CH_2-CH_2-CH_2-SO_3. The peak at 4.08 ppm could correspond to the H chemical shift of -COO-CH_2-[33]; ^1H NMR and FTIR indicated that the product contained functional groups of the monomers. The molecular structure aligned with the design, confirming the successful polymerization of RMFL.

As shown in Figure 5(c), the number-average molecular weight (M_n) of RMFL was 897940 Da, and the weight-average molecular weight (M_w) was 1176302 Da. The polydispersity index (PDI) was 1.31081, indicating a narrow molecular weight distribution and good polymerization efficiency, which helped to minimize experimental errors. The thermogravimetric (TGA) curve of RMFL is shown in Figure 5(d). As the temperature increased from 50 °C to 550 °C, the weight loss of RMFL was mainly divided into three stages. The first stage was from 50 to 197 °C, resulting in approximately 4.88% mass reduction. The mass loss was primarily due to the evaporation of bound water adsorbed on amide and sulfonic acid groups, as well as free water between the polymer chains. The second stage was from 197 to 475 °C; approximately 83.50% mass reduction was observed, primarily due to the thermal degradation of amide, sulfonic acid, the quaternary ammonium cation, and methyl groups. The third stage was from 475 °C to 550 °C; RMFL exhibited less mass loss, with a decrease of

 doi:10.20944/preprints202602.1654.v1

1.87%. During this stage, the backbone of RMFL underwent scission until the polymer was completely carbonized.

The microtopography of RMFL is shown in Figure 5(f)-(h). From Figure 5(f), RMFL displayed a fine and willow-branch-like structure under 0% NaCl conditions, which can be attributed to the electrostatic attraction between the anionic and cationic groups on the polymer side chains. The electrostatic attraction led to the contraction of the side chains. In Figure 5(g), the side chains of RMFL become extended under 36% NaCl conditions. Because the electrostatic attraction between quaternary ammonium cations and sulfonate groups was shielded by a large amount of Na^+. Furthermore, under saturated salt conditions, the network structure formed by RMFL was observed in Figure 5(h), which may result from intermolecular electrostatic and hydrophobic interactions among RMFL molecules, with electrostatic interactions being dominant. Such a network structure contributes to the regulation of the rheological properties of clay-free water-based drilling fluids.

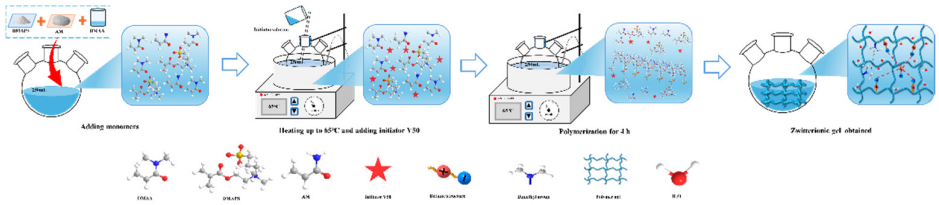

Figure 4. Synthesis of RMFL.

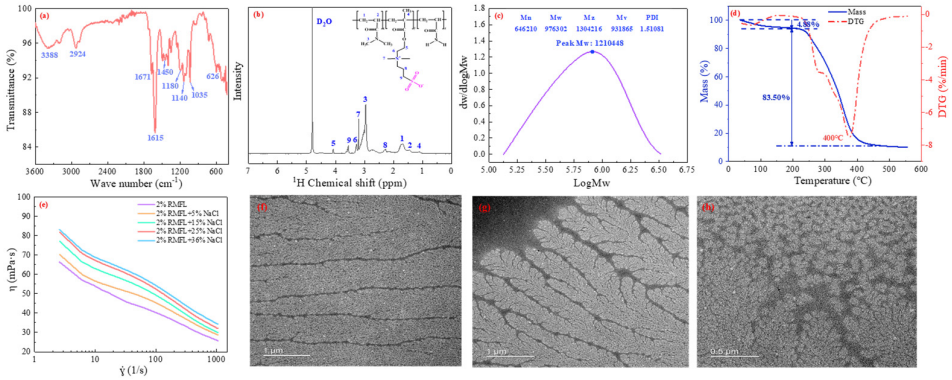

Figure 5. Characterization of RMFL. (a) FTIR; (b)1H NMR; (c) Molecular weight of RMFL;(d) TGA analysis; (e) Rheological curves of RMFL/CFWBDFs with different concentrations of NaCl. (f)-(h) Microtopography of RMFL.

2.4. Effect of Polyethyleneimine on the Performance of RMFL

The performance of the RMFL crosslinked with PEI of different molecular weights, configurations, and concentrations (w/v) is illustrated in Figure 6. As shown in Figure 6(a)-(d), increasing $LPEI_x$ concentration gradually raised the AV, PV, and YP of the RMFL($LPEI_x$)/CFWBDFs after aging at 180 °C for 16h. The FLAPI gradually decreased. Higher $LPEI_x$ concentrations led to increased crosslinking between RMFL and $LPEI_x$, enhancing the rheological properties of the RMFL($LPEI_x$)/CFWBDFs and reducing filtration loss.

$LPEI_x$ with different molecular weights exhibited different crosslinking effects at the same concentration. At 0% NaCl, $LPEI_{1800}$ demonstrated optimal crosslinking with RMFL, as the RMFL($LPEI_{1800}$)/CFWBDFs achieved the highest AV, PV, and YP after aging at 180 °C, along with the lowest FL_{API}. This difference arises because the three $LPEI_x$ have different molarity at the same concentration. The molarity of $LPEI_{1800}$ was 2.22×10^{-3} mol/L. And the molarity of $LPEI_{10000}$ was 0.4×10^{-3} mol/L, whereas the molarity of $LPEI_{70000}$ was only 0.057×10^{-3} mol/L. Although $LPEI_{1800}$ has a lower molecular weight, its molar concentration is more than five times that of $LPEI_{10000}$ and thirty-nine times that of $LPEI_{70000}$. This indicated that the molarity of the crosslinker is the primary factor

 doi:10.20944/preprints202602.1654.v1

influencing the crosslinking efficiency in freshwater environments, and it has a greater impact than molecular weight.

But $LPEI_{10000}$ was the most effective in crosslinking with RMFL under 36% NaCl conditions. This is because the longer polymer chains of $LPEI_{10000}$ can simultaneously interact with multiple RMFL chains, facilitating binding and the formation of a more extensive three-dimensional network. In high salinity environments, electrostatic interactions are strongly screened, so the crosslinking efficiency is mainly determined by the chain length and spatial bridging ability. Therefore, although $LPEI_{1800}$ has a higher molar concentration, its shorter chain length limits the number of effective crosslinking sites.

As shown in Figure 6(e)-(h), with increasing $BPEI_y$ concentration, the AV, PV, and YP of the RMFL($BPEI_y$)/CFWBDFs gradually increased after aging at 180 °C. The RMFL($BPEI_y$)/CFWBDFs exhibited higher AV, PV, and YP, with the lowest FLAPI. $BPEI_y$ demonstrated a superior crosslinking effect compared to $LPEI_x$. The results were attributed to the branched structure of $BPEI_y$. $BPEI_y$ exposed a greater number of highly reactive imine groups at the terminal ends of side chains, thereby increasing the probability of reaction with RMFL. Therefore, $BPEI_y$ was more effective than $LPEI_x$ in crosslinking with RMFL [34], significantly improving the rheological properties of RMFL($BPEI_y$)/CFWBDFs under high-temperature and high-salinity conditions.

Comparing the effects of $BPEI_y$ with different molecular weights on the RMFL($BPEI_y$)/CFWBDFs, $BPEI_{10000}$ exhibited the most effective crosslinking with RMFL under both 0% NaCl and 36% NaCl conditions. The RMFL($BPEI_{10000}$)/CFWBDFs showed the highest AV, PV, and YP, and the lowest FL_{API} after aging. This is the combined effect of molecular configuration, molecular weight, and molarity. The crosslinking efficiency of $BPEI_{70000}$ was lower because of its lower molarity at the same concentration. When the molar concentrations were comparable, such as between $BPEI_{1800}$ and $BPEI_{10000}$, a higher molecular weight may lead to improved crosslinking performance. Under saturated NaCl conditions, $BPEI_{1800}$ and $BPEI_{10000}$ were subject to strong charge screening. However, due to its higher molecular weight and larger hydrodynamic volume, $BPEI_{10000}$ exhibited stronger bridging ability and could simultaneously interact with multiple RMFL chains. In contrast, the smaller hydrodynamic volume of $BPEI_{1800}$ limited it to localized, single-point interactions.

As shown in Figure 6(i)-(l). When the $BPEI_{10000}$ concentration was 0.05%, the RMFL($BPEI_{10000}$)/CFWBDFs formed a dilute solution with good fluidity after aging at 180 °C. At a $BPEI_{10000}$ concentration of 0.10%, the RMFL($BPEI_{10000}$)/CFWBDFs became thicker after aging, exhibiting wall-clinging, easy-flow and possessed weak gel-like properties.

At a $BPEI_{10000}$ concentration of 0.15%, RMFL and $BPEI_{10000}$ created a gel with a stronger internal network. A “spitting tongue” phenomenon demonstrated significant flow resistance during pouring [35]. At a $BPEI_{10000}$ concentration of 0.20%, the internal network of the crosslinked polymer became even stronger, forming a cohesive gel. The results indicated that at $BPEI_{10000}$ concentrations of 0.10% or higher, the crosslinked polymer network was sufficiently robust to form a solid gel. It was always better to ensure adequate fluid flow during drilling rather than allow solid gel formation. Solid gel formation can cause serious problems, such as drill bit embedding, difficulty pumping fluids, and inefficient rock penetration. In summary, the optimal $BPEI_{10000}$ concentration was 0.10%. When 0.10%(m/V) $BPEI_{10000}$ was crosslinked with 2% RMFL, it did not form a soft gel. Still, it effectively increased the AV, PV, and YP of CFWBDFs under 180 °C and 36% NaCl conditions.

 doi:10.20944/preprints202602.1654.v1

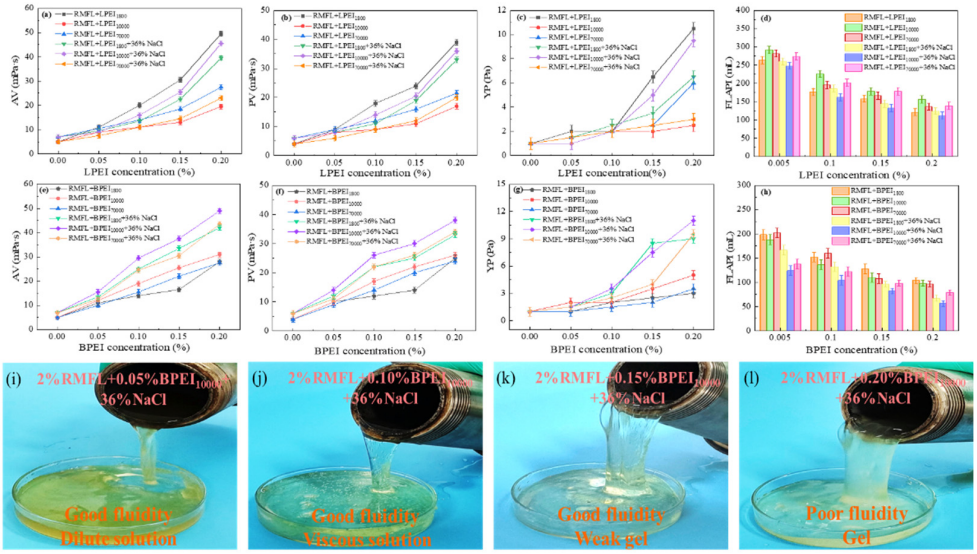

Figure 6. Effect of polyethyleneimine on the performance of RMFL. (a)-(d) Effct of $LPEI_x$ on the performance of RMFL($LPEI_x$)/CFWBDFs; (e)-(h) Effct of BPEIy on the performance of RMFL($BPEI_y$)/CFWBDFs; (i)-(l) State of RMFL($BPEI_{10000}$)/CFWBDFs with different concentration of $BPEI_{10000}$.

2.5. Rheological Properties Evaluation of RMFL($BPEI_{10000}$)/CFWBDFs

The rheological curves of the RMFL($BPEI_{10000}$)/CFWBDFs before and after aging at 180 °C under different NaCl conditions are shown in Figure 6(a)-(e). With increasing NaCl concentration, the viscosity of the RMFL($BPEI_{10000}$)/CFWBDFs gradually increased before aging, confirming the anti-polyelectrolyte effect of RMFL. After aging at 180 °C, the viscosity of the RMFL($BPEI_{10000}$)/CFWBDFs showed an initial increase, followed by a decrease, then a renewed increase. Under 5% NaCl conditions, the viscosity of the RMFL($BPEI_{10000}$)/CFWBDFs reached its highest within the shear rate range of 0–1050 s^{-1}. As the NaCl concentration increased to 36%, the viscosity of the RMFL($BPEI_{10000}$)/CFWBDFs did not decrease significantly after aging at 180 °C. The results indicated that the RMFL($BPEI_{10000}$)/CFWBDFs exhibited temperature resistance and salt tolerance.

The viscoelastic properties of the RMFL($BPEI_{10000}$)/CFWBDFs are shown in Figure 6(f)-(g). Within the shear stress range of 0.001 to 0.006 Pa, G′ consistently exceeded G′′, indicating the RMFL($BPEI_{10000}$)/CFWBDFs mainly exhibited elastic properties. When shear stress exceeded 0.07 Pa, G′′ surpasses G′, revealing primarily viscous properties. The results indicated that the RMFL($BPEI_{10000}$)/CFWBDFs was a kind of viscoelastic fluid. Intermolecular forces, such as electrostatic forces and hydrogen bonds, created a network structure between polymer chains. At low shear stress, the network could recover from disturbances, demonstrating elasticity and effectively suspending rock cuttings when static. When the shear stress increased to a certain point, the three-dimensional network experienced irreversible damage. As a result, the RMFL($BPEI_{10000}$)/CFWBDFs transferred from static to flowing, facilitating bottomhole cleaning and enhancing rock fracturing efficiency [36].

The thixotropy of the RMFL($BPEI_{10000}$)/CFWBDFs was shown in Figure 6(h)-(i). At a NaCl concentration of 36%, the viscosity of the RMFL($BPEI_{10000}$)/CFWBDFs was 117.07 mPa·s. At the shearing rate of 600 s^{-1}, the viscosity decreased to 51.48 mPa·s. When the shear rate was restored to 1 s^{-1}, the viscosity was 103.33 mPa·s, with a viscosity recovery rate of 88.26%. After aging, the RMFL($BPEI_{10000}$)/CFWBDFs with 36% NaCl exhibited a viscosity of 95.22 mPa·s at 1 s^{-1}. At the shear rate of 600 s^{-1}, the weak gel structure in the solution was disrupted, and the viscosity was reduced to 45.41 mPa·s. After the shearing rate was restored to 1 s^{-1}, the viscosity recovered to 94.34 mPa·s, representing a recovery rate of 99.07%. The results demonstrated that RMFL($BPEI_{10000}$)/CFWBDFs exhibited thixotropy under high-temperature and high-salinity conditions. The internal network was

 doi:10.20944/preprints202602.1654.v1

broken at high shearing rates, causing viscosity reduction and enabling drilling fluids to be ejected from the drill bit to break rocks and perform wellbore cleaning. The internal network structure rapidly recovered at low shearing rates, allowing drilling fluids to suspend and transport bit cuttings effectively [37].

The results demonstrated that RMFL synergized with $BPEI_{10000}$ to effectively enhance the rheological properties of RMFL($BPEI_{10000}$)/CFWBDFs. The RMFL($BPEI_{10000}$)/CFWBDFs possessed suitable viscoelasticity, thixotropy, shear-thinning behaviour, and appropriate AV, PV, and YP for RMFL($BPEI_{10000}$)/CFWBDFs, ensuring safe and efficient deep well drilling operations.

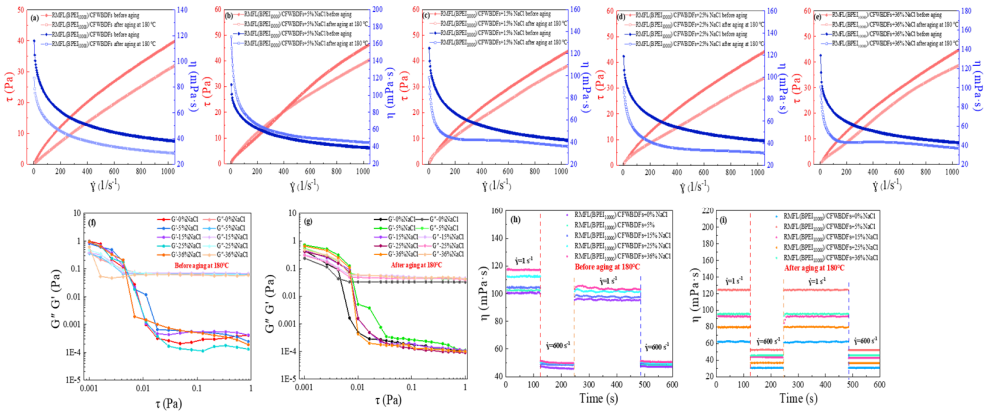

Figure 6. Evaluation of rheological properties of RMFL($BPEI_{10000}$)/CFWBDFs. (a)-(e) Rheograms of the RMFL($BPEI_{10000}$)/CFWBDFs with different concentrations of NaCl before and after aging at 180 °C.(f)-(g) Viscoelasticity analysis;(c)-(d) Thixotropy analysis.

Figure 7(a)-(d) illustrates the rheological properties and filtration loss of the RMFL($BPEI_{10000}$)/CFWBDFs under different NaCl concentrations. As the NaCl concentration increased from 0% to 36%, the PV of the RMFL($BPEI_{10000}$)/CFWBDFs was stable at 37.0 mPa·s before aging. And the PV was 31.0, 40.0, 33.0, 23.0, and 32.0 mPa·s after aging at 180 °C, with PV retention rates exceeding 60%. In contrast, the RMFL/CFWBDFs without $BPEI_{10000}$ exhibited PV less than 10.0 mPa·s. The YP of the RMFL($BPEI_{10000}$)/CFWBDFs was approximately 13.5 Pa before aging. The YP was higher than 4.0 Pa after aging. Without $BPEI_{10000}$, the YP of the RMFL/CFWBDFs was only 1.0 Pa. In terms of filtration performance, when the NaCl concentration was 5%, 15%, 25%, and 36%, the FL_{API} of RMFL ($BPEI_{10000}$)/CFWBDFs after aging were 156.6, 122.2, 143.0, 170.8 and 144.6 mL. In contrast, in the absence of $BPEI_{10000}$, the RMFL/CFWBDFs exhibited complete fluid loss during the API filtration test. The results indicated that $BPEI_{10000}$ and RMFL effectively modified the rheological behaviour and filtration performance of RMFL ($BPEI_{10000}$)/CFWBDFs.

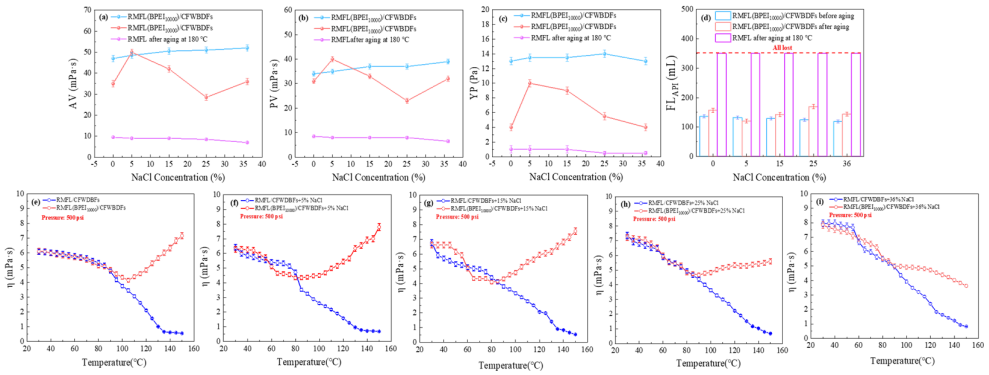

Figure 7. Rheological properties of RMFL($BPEI_{10000}$)/CFWBDFs with different concentrations of NaCl before and after aging at 180 °C. (a)-(b) AV, PV, YP and FLAPI of RMFL($BPEI_{10000}$)/CFWBDFs. (e)-(i) The viscosity-temperature curves for the RMFL($BPEI_{10000}$)/CFWBDFs from 30 °C to 150 °C at 500psi.

 doi:10.20944/preprints202602.1654.v1

The viscosity-temperature curves of RMFL(BPEI$_{10000}$)/CFWBDFs are shown in Figure 7(e)-(i). The viscosity of the RMFL/CFWBDFs decreased significantly with temperature increasing from 30 °C to 150 °C. RMFL degraded severely and could not maintain the viscosity of CFWBDFs in the absence of BPEI$_{10000}$. After adding BPEI$_{10000}$, the viscosity of the RMFL(BPEI$_{10000}$)/CFWBDFs first decreased, then increased within the NaCl concentration range of 0% to 25%, with transition temperature points at 115, 118, 128, and 132 °C, respectively. Under 36% conditions, no transition temperature was observed. The viscosity of the RMFL(BPEI$_{10000}$)/CFWBDFs gradually decreased. However, due to the crosslinking interaction between BPEI$_{10000}$ and RMFL, the viscosity of the RMFL(BPEI$_{10000}$)/CFWBDFs remained stable at 3.63 mPa·s at 150 °C and 500 psi, which was increased compared to the RMFL/CFWBDFs without BPEI$_{10000}$. As NaCl concentration increased, the crosslinking temperature of BPEI$_{10000}$ with RMFL shifted towards higher temperatures. It could result in the charge-shielding effect of Na^+ on both BPEI$_{10000}$ and RMFL, inhibiting the crosslinking reaction between BPEI$_{10000}$ and RMFL. However, the fully extended RMFL retained effective crosslinking capability with BPEI$_{10000}$, thereby improving the rheological properties of the RMFL(BPEI$_{10000}$)/CFWBDFs under high-temperature, high-salinity conditions.

2.6. Evaluation of RMFL(BPEI$_{10000}$)/CFWBDFs Under High-Density Conditions

The results are shown in Figure 8. As illustrated in Figure 8(a)-(c), the AV, PV, and YP of the drilling fluid gradually decreased with increasing density. When the drilling fluid density was 1.40 g/cm³, the PV dropped sharply to 13.0 mPa·s after aging, and the YP was only 1.0 Pa. At a density of 1.60 g/cm³, the PV further decreased to 9.0 mPa·s after aging, with the YP reduced to only 0.5 Pa. It was suggested that the crosslinking efficiency between RMFL and BPEI$_{10000}$ was weakened with increasing drilling fluid density, thereby diminishing the rheological enhancement effect of the crosslinking polymer. The phenomenon was mainly due to barite, a large inert solid particle, which created pronounced steric hindrance within the drilling fluids, interfering with effective crosslinking between RMFL and BPEI$_{10000}$.

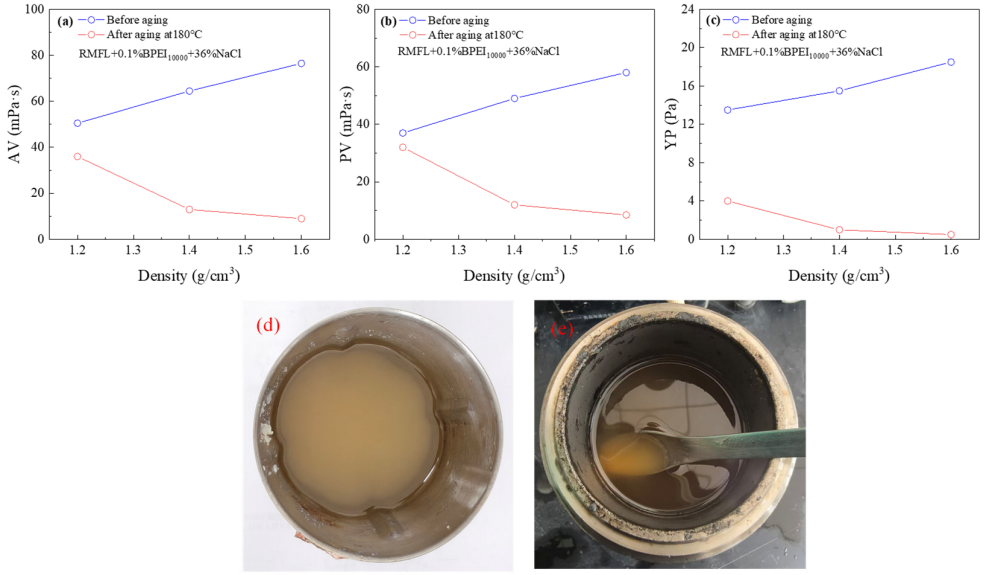

Figure 8. Influence of density on the crosslinking behaviour of RMFL and BPEI$_{10000}$.

As discussed previously, increasing the molar concentration of BPEI$_{10000}$ can enhance the crosslinking efficiency between RMFL and BPEI$_{10000}$. Therefore, the RMFL/BPEI$_{10000}$ ratio was optimised for high-density drilling fluids, and an appropriate ratio suitable for high-density barite-weighted systems was identified. For RMFL(BPEI$_{10000}$)/CFWBDFs with a density of 1.40 g/cm³, the recommended mass ratio of RMFL to BPEI$_{10000}$ was 1:0.10. When the density is increased to 1.60 g/cm³,

 doi:10.20944/preprints202602.1654.v1

the recommended mass ratio of RMFL to $BPEI_{10000}$ was 1:0.15. For RMFL ($BPEI_{10000}$)/CFWBDFs with densities of 1.80 and 2.00 g/cm3, the recommended mass ratios of RMFL to $BPEI_{10000}$ were 1:0.25 and 1:0.50. After optimization of the RMFL/$BPEI_{10000}$ ratio, the basic properties of RMFL ($BPEI_{10000}$)/CFWBDFs under saturated salt conditions before and after ageing at 180 °C are shown in Figure 9. It could be observed that RMFL ($BPEI_{10000}$)/CFWBDFs maintained good rheological properties after aging. In addition, the presence of barite significantly reduced the filtration loss.

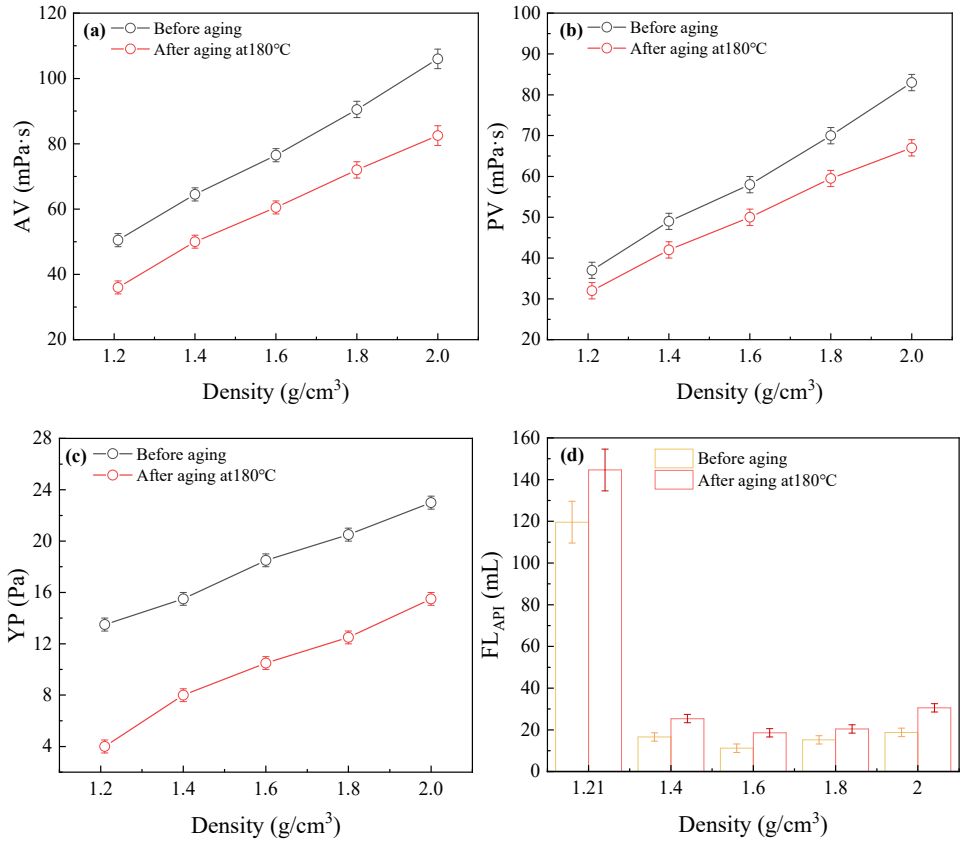

Figure 9. Performance evaluation of different density RMFL($BEPI_{10000}$)/CFWBDFs.

Further investigations were conducted to evaluate the performance of RMFL and $BPEI_{10000}$ in Ca^2-based CFWBDFs. The concentrations of RMFL and $BPEI_{10000}$ were fixed at 2.0%, 0.1%, as shown in Figure 9. From Figure 9(a), it was shown that the appearance of the $CaCl_2$ drilling fluid with a density of 1.26 g/cm³ after aging at 180 °C. Bulk insoluble aggregates were observed. Large insoluble precipitates were observed in all $CaCl_2$ drilling fluids with densities of 1.35, 1.41, and 1.43 g/cm³, as shown in Figure 9(b)、(c) and (d). As shown in Figure 9(e)-(h), the same phenomenon was also observed in $CaBr_2$ drilling fluids of different densities. With increasing amounts of $CaCl_2$ and $CaBr_2$, more precipitates formed, and the viscosity of CFBWDFs decreased to a nearly negligible level. This was because $BPEI_{10000}$ not only formed a crosslinked polymer network with RMFL but also chelated Ca^{2+}. The crosslinked polymer could adsorb a significant amount of Ca^{2+}. The abundant Ca^{2+} could strongly chelate with other crosslinked polymers, leading to extensive polymer adsorption. A large, insoluble, complex precipitate eventually formed.

The unsuitability of the RMFL/$BPEI_{10000}$ system in Ca^{2+}-based CFWBDFs indicated that the crosslinker must possess specific crosslinking functionality. It should selectively target and react with the intended polymer to form a crosslinked network, rather than reacting with other components in the system. Otherwise, the interactions with other components will undermine the effectiveness of both the polymer and the crosslinker, leading to failure of rheological regulation.

 doi:10.20944/preprints202602.1654.v1

Figure 10. Compatibility of the RMFL($BPEI_{10000}$)/CFWBDFs with Ca^{2+} and Mg^{2+}. (a)-(d) Compatibility of $BPEI_{10000}$ with different concentrations of calcium chloride; (e)-(h) Compatibility of branched polyethyleneimine with different concentrations of calcium bromide.

2.7. Mechanism Exploration

The infrared spectrum of the crosslinked polymer is shown in Figure 11(a). The broad characteristic peaks at 3545 and 3446 cm^{-1} should originate from the stretching vibrations of hydroxyl, amine, and amide groups. After RMFL crosslinking with $BPEI_{10000}$, the crosslinked polymer contained abundant amine groups. Hydrogen bonding interactions between amine groups, carboxyl, and amide groups gave rise to the broad characteristic peaks observed [38]. The characteristic peaks at 2924, 2945, and 2933 cm^{-1} were related to the asymmetric stretching vibrations of the C-H bonds in the methylene groups. The characteristic peaks at 2870, 2864, and 2860 cm^{-1} came from the symmetric stretching vibrations of the C-H bonds in the methylene groups. The characteristic peak intensity and peak area associated with methylene stretching vibrations in the cross-linked product of RMFL and $BPEI_{10000}$ were greater, indicating an increased number of methylene groups. The characteristic peak at 1681 cm^{-1} corresponded with the stretching vibration of the C=O bond in the amide group, while the peaks at 1723 cm^{-1} and 1702 cm^{-1} likely stem from the stretching vibration of the C=O bond in the carboxyl group. The amide groups might have undergone prolonged high-temperature hydrolysis, forming carboxyl groups [39]. The peaks at 1554 cm^{-1} and 1323 cm^{-1} resulted from coupled vibrations of the N-H and C-N bonds in the amine groups. After interaction between RMFL and $BPEI_{10000}$, the intensities of these peaks for the N-H and C-N bonds significantly increased. The peak at 1040 cm^{-1} originated from the stretching vibration of the C-N bond. Its intensity in the cross-linked product was notably enhanced. The crosslinked polymer exhibited detectable C=O, -OH, C-H, C-N, and N-H bonds, suggesting a marked increase in carboxyl, imine, amide, and methylene groups. The results confirmed that $BPEI_{10000}$ and RMFL underwent crosslinking under 0% and 36% NaCl conditions [40]. The zeta potential of the crosslinked polymer was measured to analyse the charge properties of the RMFL/$BPEI_{10000}$ crosslinked polymer. As shown in Figure 11(b), RMFL contained betaine-type zwitterionic structures, with sulfonate groups hydrating to carry a negative charge [41]. Due to the compressive effect of Na^+ on the double electric layer of polymers, the Zeta potential of RMFL gradually decreased. At different NaCl concentrations, the RMFL molecular chains carried negative charges before and after aging at 180 °C. It suggested that the crosslinked polymer carried a negative charge, mainly due to carboxyl groups produced by the high-temperature hydrolysis of amide groups. The decrease in zeta potential indicated an increase in negative charge on the crosslinked polymer, which improved the dispersion stability of polymers, nanoparticles, and clay during drilling operations, thereby enhancing the colloidal stability of drilling fluids [42].

 doi:10.20944/preprints202602.1654.v1

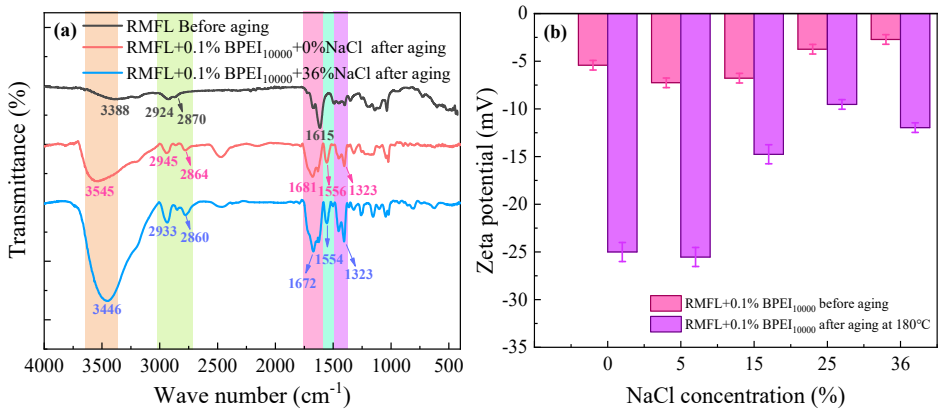

Figure 11. Characterization and analysis of the crosslinked polymer of RMFL and BPEI$_{10000}$. (a)Infrared spectrum of the crosslinking polymer; (b) Zeta potential of the crosslinked polymer.

The microstructure of the polymers was shown in Figure 12(a) and (d). Under 0% NaCl conditions, RMFL exhibited a willow-like morphology. Under 36% NaCl conditions, RMFL exhibited a densely crosslinked three-dimensional network structure. A three-dimensional network structure was observed in the crosslinked weak gel. As shown in Figure 12(e) and (f), without BPEI$_{10000}$ addition, RMFL underwent severe thermal degradation, with polymer chains visibly shortening and diminishing in size. The results demonstrated that RMFL was crosslinked with BPEI$_{10000}$ via a transamidation reaction under high-temperature stimulation, forming an extended crosslinking network weak gel. The crosslinking polymer could effectively enhance viscosity, increase shear strength, improve rheological properties, and reduce filtration loss in RMFL(BPEI$_{10000}$)/CFWBDFs under high-temperature, high-salinity conditions.

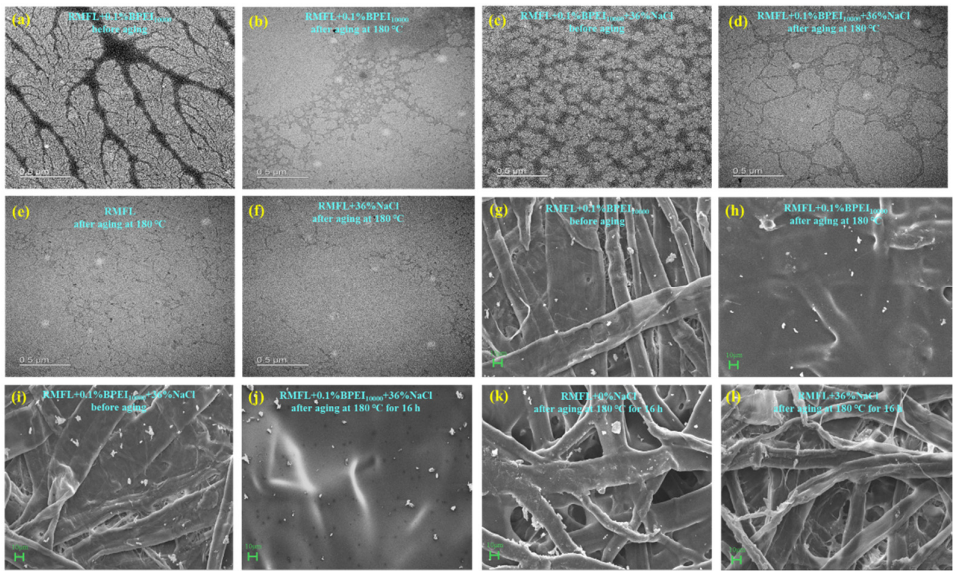

Figure 12. Analysis of polymer microtopography and Filter cake microstructure. (a)-(f) Microstructure of RMFL and crosslinked polymer;(g)-(l) Microstructure of filter cakes.

The microstructure of the filter cakes is shown in Figure 12(g)-(l). Under 0% NaCl conditions, RMFL chains were tightly packed, forming a dense filter cake with fewer apparent pores or cracks. After adding BPEI$_{10000}$, the filter cake surface remained flat, smooth, and dense after aging at 180 °C.Under 36% NaCl conditions, the RMFL(BPEI$_{10000}$)/CFWBDFs formed compact filter cakes that were smooth and devoid of discernible dehydration pores or fissures before and after aging at 180 °C. In contrast, RMFL experienced severe thermal hydrolysis in the absence of BPEI$_{10000}$, resulting in filter

 doi:10.20944/preprints202602.1654.v1

cakes with larger micropores and higher filtration losses. The results indicated that RMFL could form a crosslinked weak gel with a three-dimensional network structure synergistic with $BPEI_{10000}$. The crosslinking polymer helped form a dense mud cake and effectively reduced filtration loss.

3. Conclusions

To address the challenge of insufficient temperature and salt resistance of clay-free rheology modifiers, thermal-induced crosslinking of RMFL and $BPEI_{10000}$ was achieved through transamidation reaction, maintaining the rheological properties and reducing the filtration loss of the RMFL($BPEI_{10000}$)/CFWBDFs under conditions of 180 °C and 36% NaCl effectively. Here are the conclusions:

(1) Incorporating DMAA as the polymer backbone could endow rigidity and weak hydrophobic association properties to the polymers, and introducing DMAPS into the polymer side chains endowed the polymer with an anti-polyelectrolyte effect. The combination of DMAM and DMAPS could enhance the salt resistance of polymers.

(2) The polymers without amide groups failed to crosslink with $LPEI_{1800}$ under high-temperature and high-salinity conditions. Branched polyethyleneimine exhibited a superior cross-linking effect with RMFL compared to linear polyethyleneimine. $BPEI_{10000}$ demonstrated the most effective cross-linking performance.

(3) Under 180 °C and different NaCl conditions, the RMFL($BPEI_{10000}$)/CFWBDFs exhibited appropriate shear thinning, viscoelasticity, and thixotropy properties. In particular, the viscosity of the RMFL($BPEI_{10000}$)/CFWBDFs could be enhanced under high-temperature, high-pressure, and high-salinity conditions.

(4) A crosslinking polymer with a three-dimensional network could be formed by RMFL crosslinking with $BPEI_{10000}$, which improved the rheological properties of CFWBDFs.

(5) By synthesising salt-tolerant polymers and selecting suitable crosslinking agents, the rheological properties of clay-free water-based drilling fluids can be regulated under high-temperature and high-salinity conditions.

Study limitations and recommended future work:

(1) The crosslinking between RMFL and $BPEI_{10000}$ in this study is not easy to control.

(2) The RMFL/$BPEI_{10000}$ system was not suitable for Ca^{2+} or Mg^{2+} based CFWBDFs, as these ions readily react with $BPEI_{10000}$.

(3) The proposed approach places high demands on drilling fluid formulation, requiring that the crosslinker and polymer exhibit high selectivity and do not react with other additives.

(4) Future research should focus not only on developing high-temperature and salt-resistant polymers, but also on designing crosslinkers that are compatible with the polymers, exhibit controllable crosslinking, and have good compatibility with other drilling fluid additives. Although this approach is challenging, it remains an effective strategy to improve the overall performance of drilling fluids.

4. Materials and Methods

4.1. Materials

N, N-Dimethylacrylamide (DMAA, 99%), [2-(Methacryloyloxy)ethyl]dimethyl-(3-sulfonylpropyl)ammonium hydroxide (DMAPS, 97%), Acrylamide (AM, 99%), and 2,2′-Azobis(isobutyronitrile) dihydrochloride (V50, 97%) were procured from Shanghai Aladdin Biochemical Technology Co., Ltd. (Shanghai, China). Calcium chloride (CaCl2, 99%) and calcium bromide (CaBr2,95%) were bought from Sinopharm Group(Shanghai, China). Sodium chloride (NaCl, 99%) was purchased from McLean Biochemical Co., Ltd. (Shanghai, China). Barite was bought from the BCL group (Guangxi, China). Linear polyethyleneimine ($LPEI_x$, where x indicates the molecular weight of linear polyethyleneimine, x=1800, 10000, 70000) and branched

 doi:10.20944/preprints202602.1654.v1

polyethyleneimine ($BPEI_y$, where y indicates the molecular weight of branched polyethyleneimine, y=1800, 10000, 70000) were obtained from Beijing Konojet Energy Environmental Protection Co., Ltd.

4.2. Methods

4.2.1. Preparation of Polymers

Polyacrylamide (PAM) was synthesized using the following method: firstly, 30.0 g of AM was dissolved in 45.0 g of deionised water with stirring until complete dissolution. The solution was transferred to a three-neck flask, heated to 45 °C. And then, 0.020 g of V50 was added to the three-neck flask to initiate radical polymerization. The reaction was carried out under nitrogen for 4 hours, obtaining a transparent gel. The product was washed twice with anhydrous ethanol, dried at 80 °C for 24 hours, and ground into powder to obtain polyacrylamide (PAM). Poly(N,N-dimethylacrylamide) (PDMAA) was prepared identically to PAM, with a reaction temperature of 70 °C.

The zwitterionic modified poly(N,N-dimethylacrylamide) (PDMASs) was synthesized from DMAM and DMAPS. The total monomer mass was 30.0 g, with a monomer mass fraction of 40.0 wt%. The mass of DMAPS made up 0.5 wt%, 1.0 wt%, 1.5 wt%, and 2.0 wt% of the total monomer mass, which was 1.5 g, 3.0 g, 4.5 g, and 6.0 g of DMAPS being added in polymerization, respectively. The reaction was conducted at 70 °C, and the initiator V50 was 0.020 g. The preparation procedure for PDMAS was the same as PAM's.

In the transamidation reaction, the amide groups served as cross-linking sites between polymers and PEI. Based on the polymerization of PDMAS, the effect of the amide group mass fraction on the crosslinking of amide-based polymers and PEI was investigated by introducing amide groups. The mass fractions of AM were 0wt%, 10wt%, 20wt%, 30wt%, and 40wt% of the total monomer mass, corresponding to additions of 0 g, 3.0 g, 6.0 g, 9.0 g, and 12.0 g, respectively. The synthesised polymers were labelled PDMASA-0, PDMASA-1, PDMASA-2, PDMASA-3, and PDMASA-4. Their synthesis process was the same as PDMASs'.

The synthesis procedure for RMFL was as follows: the monomer concentration was 50 wt%. DMAM accounted for 56.0 wt% of the total monomer mass, DMAPS for 4.0 wt%, and AM for 40.0 wt%. Firstly, 22.4 g of DMAM, 1.6 g of DMAPS, and 16.0 g of AM were added to a three-neck flask. The mixture was stirred at 400 rpm for 10 minutes, until monomers were fully dissolved. The mixture was heated to 55 °C, and 0.020 g of V50 was added to initiate radical polymerization. The reaction was carried out under nitrogen for 4 hours, yielding a transparent gel. The gel was washed twice with anhydrous ethanol, dried at 80 °C for 24 hours, and ground into powder to obtain the rheology modifier RMFL.

4.2.2. Preparation of Drilling Fluids

At 25 °C, 8.0 g of polymer was dissolved in 400.0 mL of deionized water and stirred at 8000 rpm for 20 minutes to obtain the polymer-based clay-free water-based drilling fluids (polymer/CFWBDFs).

At 25 °C, 8.0 g of polymer was dissolved in 400.0 mL of deionized water and stirred at 8000 rpm for 20 minutes. Varying amounts of NaCl (0%, 5%, 15%, 25%, and 36%) were added, and the mixtures were stirred for 10 minutes to obtain the Polymer/NaCl CFWBDFs.

At 25 °C, a specified amount of polyethyleneimine was added to 5.0 g of deionized water, with stirring to promote PEI dissolution and prepare a PEI solution. The prepared PEI solution was added to the polymer/CFWBDFs. The system was stirred for 5 minutes to prepare a composite solution, labelled as polymer($LPEI_x$)/CFWBDFs or polymer($BPEI_y$)/CFWBDFs.

To evaluate the crosslinking behaviour of RMFL and $BPEI_{10000}$ at different densities and to investigate the applicability of the RMFL/$BPEI_{10000}$ composite system in high-density drilling fluids, 220.0 g and 300.0 g of barite (300 mesh) were added to 350.0 mL of RMFL ($BPEI_{10000}$)/CFWBDFs to adjust the drilling fluid densities to 1.40 g/cm3 and 1.60 g/cm3. In this system, the concentrations of

 doi:10.20944/preprints202602.1654.v1

RMFL, $BPEI_{10000}$, and NaCl were fixed at 2.0%, 0.1%, and 36%. Specifically, 480.0 g and 560.0 g of barite were added to adjust the drilling fluid density to 1.80 and 2.00 g/cm3, respectively.

At 25 °C, 140.0, 210.0, 280.0 and 350.0g $CaCl_2$ was added into 350.0mL RMFL($BPEI_{10000}$)/CFBWDFs and the densities of RMFL($BPEI_{10000}$)/CFBWDFs was adjusted to 1.26, 1.35,1.41 and 1.43 g/cm3.At 25 °C,150.0, 300.0, 450.0, 660.0g $CaBr_2$ was added into 350.0mL RMFL($BPEI_{10000}$)/CFBWDFs and the densities of RMFL($BPEI_{10000}$)/CFBWDFs was adjusted to 1.28, 1.48,1.63 and 1.75 g/cm3.The concentrations of RMFL, $BPEI_{10000}$ were fixed at 2.0%, 0.1%, and 36%.

4.2.3. Characterization of Polymers

The IRTRacer-100 Fourier Transform Infrared Spectrometer (Shimadzu, Japan) was used to analyse the molecular structure of RMFL. The scanning range was from 460 cm^{-1} to 4000 cm^{-1} with a resolution of 4 cm^{-1}.

RMFL was dissolved in D_2O and scanned with the Bruker AV III nuclear magnetic resonance spectrometer (Bruker Corporation, Germany) to obtain the ^1H NMR spectrum.

The molecular weight of the polymer was determined using the 1260 Infinity II GPC/SEC gel permeation chromatograph (Liu et al., 2023). The chromatographic column was a hydrophilic gel-permeation column packed with a hydroxylated polymethacrylate resin, with a pore size of 8 μm. Firstly, 20 mg of RMFL was added to 10 mL of water (deionized water with 0.1M $NaNO_3$) and kept static at 25 °C for 24 h, stirring several times during the period to promote RMFL dissolution. And then, the solution was filtered using microfiltration membranes (0.22 μm) to remove insoluble polymer. Finally, the clarified solution was fed into the gel chromatography column for measurement.

The viscosity-shear rate relationship of RMFL/CFWBDFs was measured using a HAAKE rheometer (Thermo Scientific, USA) in continuous rotational scanning mode. Experiments were conducted at 25 °C with the shear rate ranging from $1s^{-1}$ to 1050 s^{-1}.

The thermal stability of RMFL in N_2 was evaluated using a TGA-2 thermogravimetric analyzer. The temperature range was 30-550 °C, and the heating rate was 10 °C/min.

The transmittance of Polymer/CFWBDFs was measured at 600 nm using a UV-3600 Plus spectrophotometer (Shimadzu, Japan), and the microtopography of polymers was characterized.

4.2.4. Evaluation of Clay-Free Water-Based Drilling Fluids

The rheological properties of CFWBDFs were evaluated by the HAAKE MARS 60 rheometer (Thermo Scientific, America).

Apparent viscosity (AV, mPa·s), plastic viscosity (PV, mPa·s), and yield point (YP, Pa) are the essential rheological parameters for drilling fluids. Readings at θ600 and θ300 were obtained using a ZNN-D6 six-speed rotor viscometer (Qingdao Tongchun Petroleum Instrument Co., Ltd., China). AV, PV, and YP were calculated with the following equations. Each sample was tested three times on different instruments, and the results were averaged from the three measurements.

API filtration loss (FL_{API}) was measured using an SD6A medium-pressure filter loss apparatus (Qingdao Tongchun Petroleum Instrument Co., Ltd., China) at 0.69 ± 0.03 MPa and 25 °C. Each sample was tested twice, and the results were averaged. Drilling fluids were placed in aging tanks. And they were transferred to a high-temperature roller oven. The drilling fluids were aging at high temperatures for 16 hours. After aging, they were cooled to room temperature, stirred at 4500 rpm for 20 minutes, and the properties were measured.

The viscosity variation of RMFL ($BPEI_{10000}$)/CFWBDFs under high-temperature and high-salinity conditions was measured using a Chandler 5550 high-temperature and high-pressure rheometer (Chandler, America). Under time–temperature superposition conditions, the effect of the crosslinking reaction between RMFL and $BPEI_{10000}$ on the rheological behaviour of RMFL ($BPEI_{10000}$)/CFWBDFs was investigated. The test temperature ranged from 30 to 150 °C, with a heating rate of 1.0 °C/min. The experiment was conducted for 120 min at 500 psi, and the shear rate was $170s^{-1}$.

 doi:10.20944/preprints202602.1654.v1

4.2.5. Mechanism Analysis

The dried crosslinking polymers were ground into powder. The functional groups of crosslinking polymers were characterised by the infrared spectrometer. The zeta potential of 2% RMFL solutions (with 0.1% $BPEI_{10000}$) was measured by using the Zetasizer Nano ZS-90 Zeta potential analyser. The microstructure of RMFL and crosslinking polymers was observed using transmission electron microscopy. The filter cakes were dried at 60 °C, and the microtopography of the filter cakes was observed using an EVO 15 scanning electron microscope (Germany, Zeiss).

Author Contributions: Taifeng Zhang: Conceptualization, original draft. Jinsheng Sun: Supervision, Funding. Kaihe Lv: Resources.Jingping Liu: Supervision, Funding. Lei Nie: Acquisition.Yufan Zheng: Methodology. Yuanwei Sun: Investigation. Ning Huang: Analysis. Delin Hou: Conceptualization.Han Yan: Investigation.Yecheng Li: Analysis.

Funding: The authors are deeply grateful to the Excellent Young Scientists Fund of the National Natural Science Foundation of China (NSFC) (No. 52322401), the National Natural Science Foundation of China (NSFC) (No. 52288101).

Data Availability Statement: Data will be made available on request.

Acknowledgments: This work was supported by the National Natural Science Foundation of China.

Conflicts of Interest: All authors declare no conflicts of interest.

References

1. Huang, X.; Sun, J.; Lyu, K.; Dong, X.; Liu, F.; Gao, C. A high-temperature resistant and high-density polymeric saturated brine-based drilling fluid. *Pet. Explor. Dev*. **2023**, 50, 1215–1224. https://doi.org/10.1016/S1876-3804(23)60460-4.
2. Gao, S.D.; Lin, D.; Li, A.; Deng, L.D.; Dong A.J.; Zhang J.H. A zwitterionic polymer filtrate reducer with enhanced anti-polyelectrolyte effect for high-temperature and high-salinity conditions. *Chem. Eng. J.* **2025.** 508. 161087. https://doi.org/10.1016/j.cej.2025.161087.
3. Patel, A.D.; Indulkar, S.; Chavan, V.; Maddheshiya, P.; Asrani, M.; Thakur, S.; Singh, A.K.; Gupta, V. Clay Free Invert Emulsion Drilling Fluid System-An Innovative Rheology Modifier Which Provides Flat Rheology for Deep Water Drilling and Viscosifier for Clay Free System. *Abu Dhabi International Petroleum Exhibition & Conference*.**2018.** 49.1. https://doi.org/10.2118/192618-ms.
4. Ali, I.; Maqsood, A.; Allah, B.; Azizullah, S. Evaluation of filtration characteristics of bentonite-free water-based mud utilizing carboxymethylated tapioca starch. *Pet. Sci. Technol.* **2024.** 1-18. https://doi.org/10.1080/10916466.20242422455.
5. Li, F.; Wang, Z.; Tian, Y.; Zhang, J. Environment Friendly Water-Based Drilling Fluid Using Natural Vegetable Gum. *Asian J. Chem*. **2013**, 25, 3651–3654. https://doi.org/10.14233/ajchem.2013.13697.
6. Liu, J. Experimental study of environmental-friendly modified cellulose as rheology modifier in clay-free water-based drilling fluids. *Fresenius Environ*. Bull. **2020**, 29, 3118–3125.
7. Ali, I.; Ahmad, M.; Bakhsh, A.; Shaikh, A. Evaluation of filtration characteristics of bentonite-free water-based mud utilizing carboxymethylated tapioca starch. *Pet. Sci. Technol*. **2025**, 43(24), 3574–3591. https://doi.org/10.1080/10916466.2024.2422455.
8. Kamal, M. S.; Sultan, A. S.; Al-Mubaiyedh, U. A.; Hussein, I. A. Review on polymer flooding: Rheology, adsorption, stability, and field applications of various polymer systems. *Polym. Rev.* 2015, *55*, 491–530. https://doi.org/10.1080/15583724.2014.982821.
9. Rabiee, N.; Rabiee, M. Molecular engineering of non-covalent interactions for controlled nanomaterial assembly: Chemical principles and materials design. Coord. *Chem. Rev.* **2025**, 545, 217005. https://doi.org/10.1016/j.ccr.2025.217005.
10. Davoodi, S.; Al-Shargabi, M.; Wood, D. A.; Rukavishnikov, V. S.; Minaev, K. M. Synthetic polymers: A review of applications in drilling fluids. *Pet. Sci.* **2024**.21: 475-518. https://doi.org/10.1016/j.petsci.2023.08.015.

 doi:10.20944/preprints202602.1654.v1

11. Zhang, X.; Jiang, G.; Xuan, Y.; Wang, L.; Huang, X. Associating Copolymer Acrylamide/Diallyldimethylammonium Chloride/Butyl Acrylate/2-Acrylamido-2-methylpropanesulfonic Acid as a Tackifier in Clay-Free and Water-Based Drilling Fluids. *Energy & Fuels* **2017**, 31, 4655–4662. https://doi.org/10.1021/acs.energyfuels.6b02599.
12. Wang, J.; Sun, J.; Huang, X.; Lv, K.; Dong, X.; Geng, Y.; Xie, S. A salt-responsive amphoteric viscosifier for high-density solid-free completion fluids with high temperature resistance, strong solubility, and high viscosity enhancement. *Geoenergy Sci. Eng.* **2024a**, 243, 213303. https://doi.org/10.1016/j.geoen.2024.213303.
13. Xie, B. Q.; Ting, L.; Zhang, Y.; Liu, C. Rheological properties of bentonite-free water-based drilling fluids with novel polymer viscosifier. *J. Pet. Sci. Eng.* **2018**, 164, 302–310. https://doi.org/10.1016/j.petrol.2018.01.074.
14. Chen, T.Q.; Chen, M.J.; Fu, C.Y. Effect of molecular weight on inhibition performance of modified polyethyleneimine as polymer corrosion inhibitor for carbon steel in neutral medium. *J. Appl. Polym. Sci.* **2022.** 139: 51922. https://doi.org/10.1002/app.51922.
15. Adewunmi, A.A.; Ismail, S.; Sultan, A.S. Crosslinked Polyacrylamide Composite Hydrogels Impregnated with Fly Ash: Synthesis, Characterization and Their Application as Fractures Sealant for High Water Producing Zones in Oil and Gas Wells. *J. Polym. Environ.* **2024.** 26: 3294-3306. https://doi.org/10.1007/s10924-018-1204-9.
16. Bai, B.J.; Zhou,J.; Yin, M.F. A comprehensive review of polyacrylamide polymer gels for conformance control. *Pet. Explor. Dev.* **2015.** 42.525-532. https://doi.org/10.1016/S1876-3804(15)30045-8.
17. Pandey, V. S.; Verma, S. K.; Yadav, M.; Behari, K. Guar gum-g-N,N′-dimethylacrylamide: Synthesis, characterization and applications. *Carbohydr. Polym.* **2014**, 99, 284–290. https://doi.org/10.1016/j.carbpol.2013.08.024.
18. Tripathy, J.; Mishra, D. K.; Yadav, M.; Behari, K. Synthesis, characterization and applications of graft copolymer (chitosan-g-N,N-dimethylacrylamide). *Carbohydr. Polym.* **2010**, 79, 40–46. https://doi.org/10.1016/j.carbpol.2009.07.026.
19. Weng, L.; Gouldstone, A.; Wu, Y.; Chen, W. Mechanically strong double network photocrosslinked hydrogels from N,N-dimethylacrylamide and glycidyl methacrylated hyaluronan. *Biomaterials* **2008**, 29, 2153–2163. https://doi.org/10.1016/j.biomaterials.2008.01.012.
20. Liu, X.; Wen, Y.; Qu, J.; Geng, X.; Chen, B.; Wei, B.; Wu, B.; Yang, S.; Zhang, H.; Ni, Y. Improving salt tolerance and thermal stability of cellulose nanofibrils by grafting modification. Carbohydr. Polym. **2019**, 211, 257–265. https://doi.org/10.1016/j.carbpol.2019.02.009.
21. Hu, H.; Hu, Y.; Weng, X. Study on filter cake removal fluid of EZFLOW weak gel drilling fluid. *Gels* **2025**, *11*, 347. https://doi.org/10.3390/gels11050347.
22. Algi, M.P.; Okay, O. Highly stretchable self-healing poly(N,N-dimethylacrylamide) hydrogels. *Eur. Polym. J.***2014**. 59: 113-121. https://doi.org/10.1016/j.eurpolymj.2014.07.022.
23. Sun, J.; Zhang, X.; Lv, K.; Liu, J.; Xiu, Z.; Wang, Z.; Huang, X.; Bai, Y.; Wang, J.; Jin, J. Synthesis of hydrophobic associative polymers to improve the rheological and filtration performance of drilling fluids under high temperature and high salinity conditions. *J. Pet. Sci. Eng.* **2022**, 209, 109808. https://doi.org/10.1016/j.petrol.2021.109808.
24. Kudaibergenov, S.; Jaeger, W.; Laschewsky, A. Polymeric betaines: Synthesis, characterization, and application. In Supramolecular Polymers Polymeric Betains Oligomers; Springer: Berlin, Heidelberg, **2006**; pp. 157–224.
25. Wang, K.; Wen, J.; Zhang, S.; Yang, L.; Yang, H.; Yu, X.; Zhang, H. Magnetic polyacrylamide-based gel with tunable structure and properties and its significance in conformance control of oil reservoirs. Colloids Surf. *A Physicochem. Eng. Asp.* **2024b**, 702, 135093. https://doi.org/10.1016/j.colsurfa.2024.135093.
26. França da Câmara, P. C.; Cavalcante de Morais, S.; do Nascimento Marques, N.; Alves de Souza, E.; da Silva Gasparotto, L. H.; de Carvalho Balaban, R. Polyacrylamide and polyethylenimine mixed hydrogels tailored with crude glycerol for conformance fluids: Gelation performance and thermal stability. *Fuel*. **2023**. 354: 129376. https://doi.org/10.1016/j.fuel.2023.129376.
27. Zhao, J.Z.; Jia, H.; Pu, W.F.; Liao, R. Influences of Fracture Aperture on the Water-Shutoff Performance of Polyethyleneimine Cross-Linking Partially Hydrolyzed Polyacrylamide Gels in Hydraulic Fractured Reservoirs. *Energy &Fuels* **2011**, 25, 2616–2624. https://doi.org/10.1021/ef200461m.

 doi:10.20944/preprints202602.1654.v1

28. Guo, H.; Ge, J.; Zhao, S.; Xu, Y.; Zhou, D.; Tao, Z. Performance evaluation of high-strength polyethyleneimine gels and syneresis mechanism under high-temperature and high-salinity conditions. *SPE J.* 2022, *27*, 3630–3642. https://doi.org/10.2118/210593-PA.
29. Luo, Y.; Lin, L.; Guo, Y.; Luo, P.; Xiong, G.; Li, Z.; Ao, H. Study on high-temperature degradation of acrylamide-based polymer ZP1 in aqueous solution. *Polym. Degrad. Stab.* **2023a**, 217, 110533. https://doi.org/10.1016/j.polymdegradstab.**2023**.110533.
30. Zhang, T.F.; Sun, J.S.; Liu, J.P.; Lv, K.H.; Sun, Y.W.; Xu, Z.; Huang, N.; Yan, H. High-temperature and high-salinity resistance hydrophobic association zwitterionic filtrate loss reducer for water-based drilling fluids. *Pet. Sci.* **2025**, 22, 2851–2867. https://doi.org/10.1016/j.petsci.2025.05.016.
31. Li, J.; Sun, J.; Lv, K.; Ji, Y.; Liu, J.; Huang, X.; Bai, Y.; Wang, J.; Jin, J.; Shi, S. Temperature- and salt-resistant micro-crosslinked polyampholyte gel as fluid-loss additive for water-based drilling fluids. *Gels.* **2022**, 8, 289. https://doi.org/10.3390/gels8050289.
32. Luo, Y.; Lin, L.; Yu, W.; Li, X.; Gu, H. Synthesis and Evaluation of Betaine Copolymer Filtrate Reducer for Drilling Mud. Clays Clay Miner. 2022, 70, 252–269. https://doi.org/10.1007/s42860-022-00181-w.
33. Sepehri, S.; Soleyman, R.; Varamesh, A.; Valizadeh, M.; Nasiri, A. Effect of synthetic water-soluble polymers on the properties of the heavy water-based drilling fluid at high pressure-high temperature (HPHT) conditions. *J. Pet. Sci. Eng.* **2018**, 166, 850–856. https://doi.org/10.1016/j.petrol.2018.03.055.
34. Lei, T.; Wang, Y.; Zhang, H.; Cao, J.; Xiao, C.; Ding, M.; Chen, W.; Chen, M.; Zhang, Z. Preparation and performance evaluation of a branched functional polymer for heavy oil recovery. *J. Mol. Liq.* **2022**, 363, 119808. https://doi.org/10.1016/j.molliq.2022.119808.
35. Baruah, U.; Manna, U. The synthesis of a chemically reactive and polymeric luminescent gel. *Chem. Sci.***2021.**12. 2097-2107. https://doi.org/10.1039/D0SC05166G.
36. Davoodi, S.; Ahmad Ramazani S.A., A.; Soleimanian, A.; Fellah Jahromi, A. Application of a novel acrylamide copolymer containing highly hydrophobic comonomer as filtration control and rheology modifier additive in water-based drilling mud. *J. Pet. Sci. Eng.* **2019**.180: 747-755. https://doi.org/10.1016/j.petrol.2019.04.069.
37. Yang, J.; Wang, R.; Sun, J.; Qu, Y.; Ren, H.; Zhao, Z.; Wang, P.; Li, Y.; Liu, L. Comb polymer/layered double hydroxide (LDH) composite as an ultrahigh temperature filtration reducer for water-based drilling fluids. *Appl. Surf. Sci.* **2024**, 645, 158884. https://doi.org/10.1016/j.apsusc.2023.158884.
38. Yang, J.; Wang, R.; Sun, J.; Wang, J.; Liu, L.; Qu, Y.; Wang, P.; Ren, H.; Gao, S.; Yang, Z. Nanolaponite/Comb Polymer Composite as a Rheological Modifier for Water-Based Drilling Fluids. *ACS Appl. Nano Mater.* **2023**, 6, 13453–13465. https://doi.org/10.1021/acsanm.3c02079.
39. Luo, Y.; Lin, L.; Luo, P.; Guo, Y.; Xie, S.; Wang, M.; Xiong, G.; Gu, H. Polymer nanocomposite ADA@SM as a high-temperature filtrate reducer for water-based drilling fluids and its filtration loss mechanism. *Colloids Surf. A Physicochem. Eng. Asp.* **2023**, 672, 131701. https://doi.org/10.1016/j.colsurfa.2023.131701.
40. Fritsch, D.; Merten, P.; Heinrich, K.; Lazar, M.; Priske, M. High performance organic solvent nanofiltration membranes: Development and thorough testing of thin film composite membranes made of polymers of intrinsic microporosity (PIMs). *J. Membr. Sci.* **2012.** 401-402: 222-231. doi: https://doi.org/10.1016/j.memsci.2012.02.008.
41. Li, J.; Ji, Y.-X.; Ni, X.-X.; Lv, K.-H.; Huang, X.-B.; Sun, J.-S. A micro-crosslinked amphoteric hydrophobic association copolymer as high temperature- and salt-resistance fluid loss reducer for water-based drilling fluids. *Pet. Sci.* **2024**, 21, 1980–1991. https://doi.org/10.1016/j.petsci.2024.01.021.
42. Liu, J.P.; Zhang, T.F.; Sun, Y.W.; Lin, D.; Feng, X.; Wang, F. Insights into the high temperature-induced failure mechanism of bentonite in drilling fluid. *Chem. Eng. J.* **2022**, 445, 136680. https://doi.org/10.1016/j.cej.2022.136680.